Journal of Crystal Growth 410 (2015) 1–6

Contents lists available at ScienceDirect

Journal of Crystal Growth

journal homepage: www.elsevier.com/locate/jcrysgro

Real structure of lattice matched GaAs–Fe_3Si core–shell nanowires

B. Jenichen *, M. Hilse, J. Herfort, A. Trampert

Paul-Drude-Institut für Festkörperelektronik, Hausvogteiplatz 5-7, D-10117 Berlin, Germany

ARTICLE INFO

Article history:
Received 16 July 2014
Received in revised form
2 October 2014
Accepted 12 October 2014
Communicated by K. Deppert
Available online 24 October 2014

Keywords:
A1 Nanostructures
A3 Molecular beam epitaxy
B1 Gallium compounds
B1 Metals
B2 Magnetic materials

ABSTRACT

GaAs nanowires and GaAs–Fe_3Si core–shell nanowire structures were grown by molecular-beam epitaxy on oxidized Si(111) substrates and characterized by transmission electron microscopy (TEM) and X-ray diffraction (XRD). Ga droplets were formed on the oxide surface, and the semiconducting GaAs nanowires grew epitaxially via the vapor–liquid–solid mechanism as single-crystals from holes in the oxide film. We observed two stages of growth of the GaAs nanowires, first the regular growth and second the residual growth after the Ga supply was finished. The magnetic Fe_3Si shells were deposited in an As-free chamber. They completely cover the GaAs cores although they consist of small grains. High-resolution TEM micrographs depict the differently oriented grains in the Fe_3Si shells. Selected area diffraction of electrons and XRD gave further evidence that the shells are textured and not single crystals. Facetting of the shells was observed, which lead to thickness inhomogeneities of the shells.

1. Introduction

Semiconductor nanowires (NWs) represent systems for exploring nanoscale physics and to design a variety of new devices (see Ref. [1] for a review). They can be grown not only on dissimilar substrates but also as axial and radial heterostructures [2–4]. Device concepts based on the spin rather than the charge of the electron have been introduced in the field of spintronics. Among these concepts, nanowires that combine a semiconductor and a ferromagnet in a core–shell geometry have gained a lot of interest since 2009 when they were presented for the first time [5–10]. Because of the cylindrical shape of the ferromagnet, such core–shell nanowires could allow for a magnetization along the wire and thus perpendicular to the substrate surface. Ferromagnetic stripes or tubes with a magnetization perpendicular to the substrate have the potential for circular polarized light emitting diodes that optically can transmit spin information in zero external magnetic field and thus allow for on-chip optical communication of spins on one hand [11]. On the other hand they enable three-dimensional magnetic recording with unsurpassed data storage capacities [12,13]. The perfect lattice matching of the binary Heusler alloy Fe_3Si and GaAs allows for the molecular beam epitaxy (MBE) growth of planar high quality hybrid structures [14–16]. In addition, the cubic Fe_3Si phase [17,18] shows a robust stability against stoichiometric variations with only slightly modified magnetic properties [19]. Moreover, its thermal stability against chemical reactions at the ferromagnet/semiconductor interface is considerably higher than that of conventional ferromagnets like Fe, Co, Ni, and Fe_xCo_{1-x} [20]. Together with the high Curie temperature of about 840 K this material system has therefore several advantages compared to most of the previously studied semiconductor-ferromagnet core–shell nanowires using ferromagnetic materials that cannot reach the high quality of a binary Heusler alloy like Fe_3Si [5–10]. Recently, we have demonstrated for the first time that GaAs–Fe_3Si core–shell NWs prepared by MBE show ferromagnetic properties with a magnetization oriented along the NW axis (perpendicular to the substrate) [21]. However, the structural properties and hence the magnetic properties of the core–shell NWs depend strongly on the substrate temperature during the growth of the Fe_3Si shell [21]. In this work, we present a detailed investigation of the real structure of both GaAs NWs and GaAs–Fe_3Si core–shell NWs using transmission electron microscopy (TEM) and X-ray diffraction (XRD).

2. Experiment

Fe_3Si–GaAs core–shell NW structures are grown by MBE on Si(111) substrates. First, GaAs nanowires are fabricated by the Ga-assisted growth mode on the Si(111) substrates covered with a thin native Si-oxide layer. The growth mechanism is the vapor–liquid–solid (VLS) mechanism [22–26], where pin holes in the SiO_2 serve as nucleation sites [4]. A Ga droplet is the preferred site for deposition from the vapor. The GaAs NW then starts to grow by preferential nucleation at the spatially restricted GaAs/Si interface (IF). Further growth is unidirectional and proceeds at the solid/liquid IF. The GaAs NWs are grown at a substrate temperature of 580 °C, and a V/III flux ratio of unity. The equivalent two-

* Corresponding author.
E-mail address: bernd.jenichen@pdi-berlin.de (B. Jenichen).

http://dx.doi.org/10.1016/j.jcrysgro.2014.10.017
0022-0248/

dimensional growth rate amounts to 100 nm/h. In order to finish the NW growth, the Ga-shutter is closed. Then the Ga-droplets on top of the NWs are consumed in the arsenic atmosphere. During this phase of the experiment there is still a certain NW growth taking place at a reduced diameter. The samples are then cooled down. Once the NW templates are grown, they are transferred under ultra high vacuum conditions to an As free growth chamber for metals of the same MBE system. There the GaAs NW templates are covered with Fe_3Si shells at different substrate temperatures ranging from 100 °C to 350 °C. More details regarding the growth conditions can be found in Ref. [21]. The main growth parameters are summarized in Table 1.

The NW structures are characterized by scanning electron microscopy (SEM), by dark-field (DF) and high-resolution (HR) TEM, selected area diffraction (SAD) of electrons and XRD. The TEM specimens are prepared by mechanical lapping and polishing, followed by argon ion milling according to standard techniques. TEM images are acquired with a JEOL 3010 microscope operating at 200 kV and 300 kV. The cross section TEM methods provide high lateral and depth resolutions on the nanometer scale, however they average over the thickness of the thin sample foil or the thickness of the NW as a whole. The resolution limit of the dark-field method with the TEM used is in the ideal case about 0.2 nm. There can be additional errors due to projection and due to curvature of the interfaces.

HR XRD measurements are performed using a Panalytical X-Pert PRO MRD™system with a Ge(220) hybrid monochromator (Cu $K\alpha_1$ radiation with a wavelength of $\lambda = 1.54056\,\AA$).

3. Results and discussion

Fig. 1 (a) shows an SEM micrograph of the pure GaAs NWs (sample 0). The micrograph of the sample surface reveals a relatively low area density of NWs of about $5 \times 10^8\,cm^{-2}$. Besides the well oriented NWs we see GaAs hillhocks [4]. During the last phase of GaAs NW growth no more Ga is supplied, and so the remaining Ga in the droplet on top of the NWs is consumed leading to a prolongation of the NW at reduced diameter. These thinner end pieces of the GaAs NWs can be recognized in Fig. 1(a). Fig. 1(b) shows a multi-beam TEM micrograph of a GaAs NW. Planar defects can be recognized near the Si/GaAs IF and near the area of diameter reduction of the NW. The other regions of the NW are free of defects.

Fig. 2(a) demonstrates a HRTEM micrograph of the Si/GaAs IF illustrating the epitaxial alignment of a GaAs NW on Si(111) (sample 0). No amorphous material (i.e. SiO_2) is observed at the GaAs/Si IF. Probably a remaining thin SiO_2 film was etched away by the Ga droplet [27]. Here, the IF is a perfect twin boundary, however, NWs without twinning at the IF are observed as well.

Fig. 2(b) displays the dark-field (DF) image of a GaAs–Fe_3Si core–shell NW taken under $g = 111$ (sample 1). The GaAs core is dark and the Fe_3Si shell region yields an inhomogeneous distribution of intensity, due to its textured structure. It fulfills the diffraction condition in correspondence to the different orientations of the individual crystallites. The shell is 18 ± 3 nm thick at the sidewall, where ± 3 nm characterizes the thickness inhomogeneity and not the error of the measurement. This thickness does not correspond to the equivalent amount of material deposited. It seems that a higher amount of the Fe_3Si is integrated into more than 60 nm thick parasitic film. The material thickness on top of the NWs is even higher (about 86 nm). The value of 86 nm corresponds to the nominal film thickness of 69 nm expected for a planar structure. The diffusion of Fe_3Si along the sidewalls can be neglected, in first approximation. Then, the reduced film thickness along the sidewalls of the NWs can be explained by the small angle between the direction of the material flux and the NWs in the MBE system. Fig. 2(c) shows the corresponding BF image of the core–shell NW shown in (b). Here, the Fe_3Si shell does not fulfil the diffraction condition, however, the single-crystalline GaAs core diffracts strongly, resulting in a high intensity of the GaAs 111 reflection. Fig. 2(b) and (c) shows clearly the reduction of the diameters of the cores after closing the Ga-shutter. Two different diameters of the GaAs cores [e.g. 50 nm and about 33 nm in Fig. 2(b) and (c)] can be recognized, evidencing two stages of NW growth.

Fig. 3(a) shows a TEM BF image of a plan-view along the axis of a GaAs–Fe_3Si core–shell NW (sample 1). The single-crystalline GaAs core exhibits an almost homogenous contrast. The shell is 26 ± 7 nm thick. The thickest regions are found at the corners. We

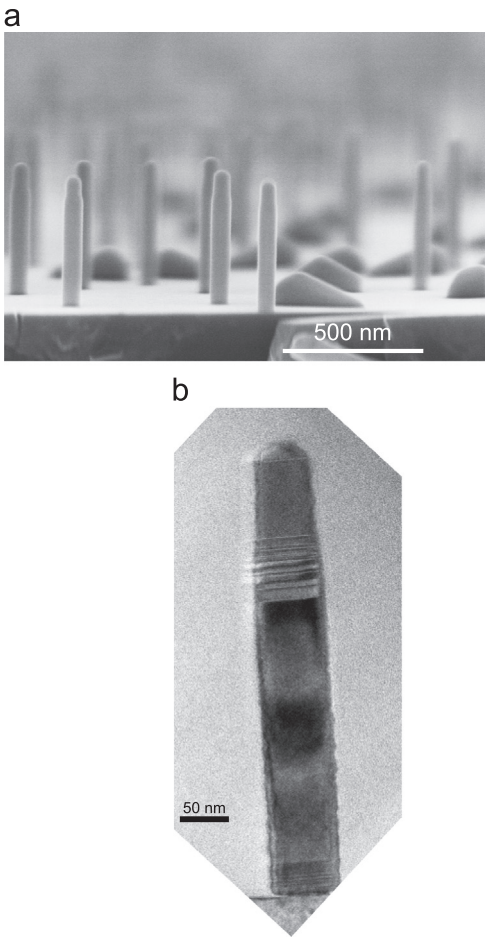

Fig. 1. (a) SEM image of GaAs NWs and GaAs islands between the NWs grown by molecular beam epitaxy on a Si(111) substrate (sample 0). The end pieces of the NWs have a smaller diameter. (b) Multi-beam TEM micrograph of a GaAs NW.

Table 1
Substrate temperatures T_S during epitaxial NW growth and equivalent film thicknesses, calculated from growth rates and deposition times for the four samples investigated.

Material	Sample thickness (nm)	No. 0, T_S (°C)	Sample thickness (nm)	No. 1, T_S (°C)	Sample thickness (nm)	No. 2, T_S (°C)	Sample thickness (nm)	No. 3, T_S (°C)
GaAs	22	580	22	580	22	580	22	580
Fe_3Si	–	–	69	100	69	200	69	350